Versatile mid-infrared frequency-comb referenced sub-Doppler spectrometer

A. Gambetta, E. Vicentini, N. Coluccelli, Y. Wang, T. T. Fernandez, P. Maddaloni, P. De Natale, A. Castrillo, L. Gianfrani, P. Laporta, and G. Galzerano

Citation: APL Photonics **3**, 046103 (2018); doi: 10.1063/1.5025135

View online: https://doi.org/10.1063/1.5025135

View Table of Contents: http://aip.scitation.org/toc/app/3/4

Published by the American Institute of Physics

APL PHOTONICS **3**, 046103 (2018)

Versatile mid-infrared frequency-comb referenced sub-Doppler spectrometer

A. Gambetta,[1,2,a] E. Vicentini,[1] N. Coluccelli,[1,2] Y. Wang,[1,2] T. T. Fernandez,[2] P. Maddaloni,[3,4] P. De Natale,[5] A. Castrillo,[6] L. Gianfrani,[6] P. Laporta,[1,2] and G. Galzerano[1,2]

[1]*Dipartimento di Fisica-Politecnico di Milano, Piazza Leonardo da Vinci 32, 20133 Milano, Italy*
[2]*Istituto di Fotonica e Nanotecnologie-CNR, Piazza Leonardo da Vinci 32, 20133 Milano, Italy*
[3]*CNR-INO, Istituto Nazionale di Ottica, Via Campi Flegrei 34, 80078 Pozzuoli (NA), Italy*
[4]*INFN, Istituto Nazionale di Fisica Nucleare, Sez. di Napoli, Complesso Universitario di M. S. Angelo, Via Cintia, 80126 Napoli, Italy*
[5]*CNR-INO, Istituto Nazionale di Ottica, Largo Enrico Fermi 6, 50125 Firenze, Italy*
[6]*Dipartimento di Matematica e Fisica-Università degli Studi della Campania "Luigi Vanvitelli," Viale Lincoln 5, 81100 Caserta, Italy*

(Received 7 February 2018; accepted 18 March 2018; published online 30 April 2018)

We present a mid-IR high-precision spectrometer capable of performing accurate Doppler-free measurements with absolute calibration of the optical axis and high signal-to-noise ratio. The system is based on a widely tunable mid-IR offset-free frequency comb and a Quantum-Cascade-Laser (QCL). The QCL emission frequency is offset locked to one of the comb teeth to provide absolute-frequency calibration, spectral-narrowing, and accurate fine frequency tuning. Both the comb repetition frequency and QCL-comb offset frequency can be modulated to provide, respectively, slow- and fast-frequency-calibrated scanning capabilities. The characterisation of the spectrometer is demonstrated by recording sub-Doppler saturated absorption features of the CHF_3 molecule at around 8.6 μm with a maximum signal-to-noise ratio of $\sim 7 \times 10^3$ in 10 s integration time, frequency-resolution of 160 kHz, and accuracy of less than 10 kHz. https://doi.org/10.1063/1.5025135

I. INTRODUCTION

The accuracy of the absolute optical frequency axis and signal-to-noise level are key parameters for any precision-spectroscopy measurement. The advent of visible and near-infrared optical frequency-combs[1,2] at the beginning of the century gave a tremendous boost to precision spectroscopy systems, allowing for a straightforward and absolute optical frequency calibration potentially reaching the 10^{-16}–10^{-18} level of the most accurate atomic and optical frequency standards today available.[3,4] Moreover, the continuous progress in Quantum-Cascade-Laser (QCL) technology recently led to the availability of room-temperature plug-and-play mid-infrared (mid-IR) single-frequency tunable laser sources with an optical power of few tens of mW, 1 MHz emission linewidth, and very high frequency stability[5–7] allowing for the detection of strong fundamental absorption lines with a high signal-to-noise ratio (SNR) and resolution. The use of QCLs combined with the more recent availability of mid-IR frequency combs[8–12] has allowed to extend precision spectroscopy to the 3-15 μm spectral window (covering the majority of the fingerprint region) where most molecules exhibit their strongest absorption features, greatly enhancing both accuracy and sensibility of direct-absorption spectroscopy measurements. Several spectroscopic techniques can also be implemented for further increase of system resolution, accuracy, and sensitivity. Non-linear spectroscopy techniques[13] allow us, for instance,

[a]Electronic mail: alessio.gambetta@polimi.it

to partially remove the sources of inhomogeneous spectral line-broadening allowing us to observe Doppler-free absorption features few orders of magnitude narrower than the linear-absorption profiles, with a strong benefit for measurement precision. Balanced detection or other well assessed background-removal techniques can also be adopted to account for baseline-related artifacts, such as etalon effects or beam-intensity wavelength dependence, that may also affect the overall accuracy. Modulation-spectroscopy techniques[14] on the other hand allow for both technical-noise and background rejection, therefore enabling for very sensitive detection, which is very important especially in the presence of very crowded absorption spectra typical of heavy molecules or molecular mixtures.

In this work, we present a versatile and relatively simple spectrometer based on a QCL laser frequency-locked to a mid-IR optical frequency comb, capable of Doppler-free precision-spectroscopy measurements with high-accuracy and high-sensitivity in both direct-absorption and modulation-spectroscopy approaches. We tested the system performances by probing narrow spectral features of trifluoromethane, CHF_3, which is a very important molecule for the emerging field of cold stable molecules[15] and which is very demanding from a spectroscopy point of view due to a very crowded absorption spectrum. With respect to our previous investigations,[16,17] in this work, we focused our attention to the analysis of sub-Doppler spectral features using a novel absolute-calibrated scanning approach which is a powerful method to retrieve several spectroscopic parameters.

II. EXPERIMENTAL SETUP

The experimental setup is sketched in Fig. 1 and is based on a commercial distributed-feedback (DFB) QCL tunable between 8.55 and 8.65 μm with a maximum optical power of ~40 mW, tightly locked to a mid-IR, difference frequency generation (DFG)-based, optical frequency-comb tunable in the region between 8 and 14 μm having a repetition frequency f_r = 250 MHz. Further details on the mid-IR comb generation setup can be found in Ref. 12. The QCL beam acts as the actual spectroscopic laser source, while the mid-IR comb serves for stabilisation and calibration purposes. The QCL output beam is collimated by a 20-cm focal length anti-reflection (AR) coated ZnSe plano-convex lens (not shown in Fig. 1) to a beam waist of 2.1 mm and split into two parts by a 50:50 beam splitter (BS_1). The reflected beam-portion is collinearly superimposed onto BS_2 with the mid-IR comb, filtered by

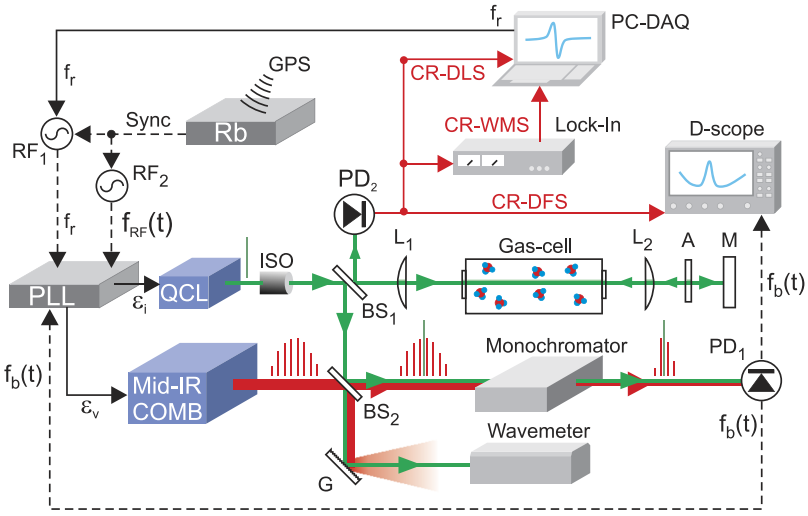

FIG. 1. Experimental setup. RF: radio-frequency signal synthesiser, ISO: optical isolator, PD: photodiode, A: attenuator, M: mirror, BS: beam splitter, L: lens, G: grating. Red arrows represent the spectroscopic signals, for each of the three adopted measurement approaches: comb-referenced direct-absorption long-scan (CR-DLS), comb-referenced wavelength-modulation scans (CR-WMS), and comb-referenced direct-absorption fast-scan (CR-DFS). QCL and COMB spectra are schematised as vertical narrow lines (green and red, respectively) along the optical path of the corresponding laser-beams, before and after recombination and after spectral filtering.

a 0.01 μm resolution monochromator and focused for beat-note detection onto a liquid-nitrogen cooled 200 MHz bandwidth mercury-cadmium-telluride (MCT) detector (PD_1, responsivity of 5.7×10^4 V/W, 50 nV/$\sqrt{\text{Hz}}$ noise floor, and 60 μW saturation power-level). The beat-note signal detected by PD_1 and its instantaneous frequency $f_b(t)$ are monitored by a 12-bit digital oscilloscope (D-scope) with real-time FFT capabilities. The beat-note signal contains information on the QCL instantaneous optical frequency ν_{QCL} which is given by $\nu_{QCL}(t) = nf_r \pm f_b(t)$, where n is the comb-mode order closest to the QCL emission line (the sign of f_b depends on whether ν_{QCL} is higher or lower than nf_r). It is worth pointing out that no contribution from the comb offset-frequency (CEO) is present since the DFG process produces a harmonic comb with a CEO constantly equal to zero. The nearest comb order n is univocally determined by measuring ν_{QCL} with an accuracy better than half mode-spacing, by means of a ±1 ppm accuracy wavemeter with an operating wavelength-range between 4 μm and 11 μm (Bristol 621B-MIR). The wavemeter is aligned onto the QCL beam portion transmitted by BS_2 (in order to avoid misreading, a grating is used to spatially filter the comb spectrum before entering the wavemeter).

Two separate phase-locked servo-loops (PLLs) are implemented to stabilise, respectively, the comb spacing f_r and the beat-note signal frequency $f_b(t)$ with respect to two distinct radio-frequency (RF) reference signals provided by a couple of low-noise RF synthesisers (respectively, RF_1 and RF_2 of Fig. 1) both synchronized to a global positioning system disciplined Rb oscillator (8×10^{-12} stability at 1 s) which distributes a 10-MHz standard clock signal over the whole setup. In particular, $f_b(t)$ is used for locking, narrowing, and calibration of the QCL emission line.

The QCL-beam portion transmitted through BS_1 is sent to a 25 cm long stainless steel cell equipped with AR-coated Zn-Se windows and filled with the gas sample to be analyzed. Beyond the cell output-window, the beam travels, respectively, through a second lens, a 50% attenuator, and a back-reflecting mirror, providing a counter-propagating weak probe beam with roughly 25% of the pump-beam power.[16] After being collinearly superimposed with the pump inside the cell, with matching phase-fronts in the middle of the cell (probe waist diameter $d_{PR} = 1.8$ mm), the probe beam is sent to a thermoelectrically cooled, 50-MHz MCT detector (PD_2) for detection. A 30 dB optical isolator placed at the output of the QCL prevents the onset of optical feedback, minimizing the portion of the beam back-reflected toward the QCL, due to the double pass arrangement. A personal computer (PC) running Matlab controls the whole instrumentation allowing to perform the spectroscopic scans. As a final remark, we would like to point out that, at the cost of a little complication to the setup, an extended-cavity QCL could be used instead,[18] extending the working range of the spectrometer to the 7-11 μm wavelength interval, limited on the lower side by the mid-IR comb tunability and on the upper side by the operative wavelength range of the wavemeter used for extrapolating the comb-mode order n.

III. MEASUREMENT APPROACHES

By recording the transmission signal detected by PD_2 as a function of the QCL absolute frequency, several kinds of Doppler-free measurements can be performed adopting three different and complementary scan approaches, as sketched in Fig. 2. A detailed description of these methods is presented in the following, pointing out advantages and drawbacks of each approach.

(1) Comb-Referenced, Direct-absorption, Long frequency-Scans (CR-DLSs) where calibrated scans of several cm^{-1} frequency span with a maximum SNR ~ 10^2 (with respect to the saturated Lamb-dip contrast) can be performed. In this configuration, the beat-note frequency, $f_b(t)$, is tightly locked to a RF signal of constant frequency f_{RF} provided by RF_2, while f_r is varied by discrete steps.[17] For each value of f_r, the spectroscopic signal from PD_2 is recorded by a 16 bit, 400 kS/s data-acquisition board (DAQ) as a function of the corresponding QCL absolute optical frequency $\nu_{QCL}(f_r)$. This simple approach requires long acquisition times (several minutes to tens of minutes per scan) and allows moderate frequency sampling intervals ($\delta\nu_{QCL}$ ~ 1 MHz), with an SNR mainly limited by the low-frequency intensity noise of the QCL.

(2) Comb-Referenced, Wavelength-Modulation frequency-Scans (CR-WMSs) where a fast modulation (up to 100 kHz) is applied to $f_{RF}(t)$ and transferred to $\nu_{QCL}(t)$ by the PLL, while the

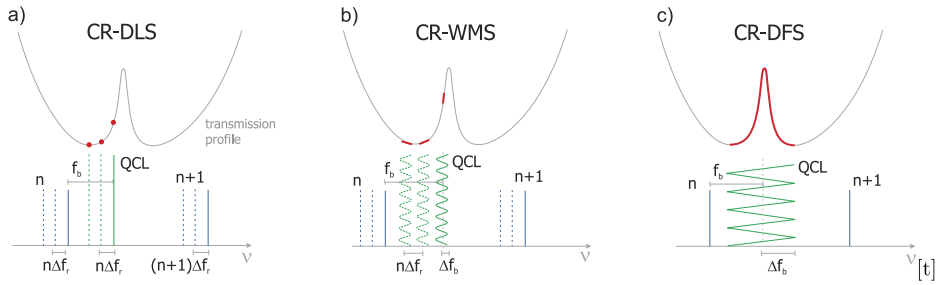

FIG. 2. Visual representation of the three measurement approach exploited. (a) The frequency-distance f_b between the QCL (green line) and the nearest comb mode (blue) n is kept fixed while the comb f_r is scanned by multiples of Δf_r. Dashed vertical lines represent previous frequency-positions along the scan, while continuous lines are the actual positions. Red dots are the transmission profile points sampled by the QCL during the scan. (b) A small frequency modulation Δf_b is applied to $f_b(t)$ while the comb f_r is scanned: for each sample point, the derivative of the absorption profile is recorded at the lock-in output (slope of the red straight-lines). (c) Comb modes are fixed while $f_b(t)$ is periodically linearly scanned across the average value f_b, with a maximum deviation of $\pm\Delta f_b$. A quasi-continuum of sample points is acquired in this configuration (red line).

transmittance signal from PD_2 is de-modulated in a lock-in amplifier. Again f_r is scanned step-by-step while the de-modulated signal is recorded as a function of $\nu_{QCL}(f_r)$. Compared to the CR-DLS, this approach grants a higher SNR ($\sim 10^3$) and background rejection while maintaining the same acquisition times. By contrast, it requires additional data-analysis efforts in order to assess spectroscopic information from the retrieved data and to take into account modulation-induced line-profile distortions.[19]

In order to achieve the above specified SNR values for CR-DLS and CR-WMS, a ~1 s wait-time per sample point is required. The typical measurement settings are therefore a compromise between the number of spectral elements acquired, frequency span, and measurement time. Considering a reasonable measurement time of about ~20 min per scan, the maximum number of resolved spectral elements is limited to ~1200. The sampling interval strictly depends on the width of the spectral features to be measured and is usually set between ~100 kHz and ~1 MHz, leading to frequency spans per single-scan from ~120 MHz to ~1.2 GHz wide.

(3) Comb-Referenced, Direct-absorption, Fast frequency-Scans (CR-DFSs) where the repetition-frequency f_r is kept fixed, while a frequency modulation in the kHz range is applied to the QCL (as in the CR-WMS method but with a larger modulation-depth, up to $f_r/4$), allowing for optical frequency scans up to $\Delta\nu_{QCL} \sim 100$ MHz. In this novel approach, the periodic transmission signal from PD_2 is sent to D-scope together with the frequency-modulation waveform, which acts as a trigger for the acquisition. Thanks to a very short single-scan acquisition-time, corresponding to the inverse of the modulation-frequency (few tens of μs), a great number of scans can be acquired and real-time averaged into a single CR-DFS measurement lasting only few seconds. This approach grants for very narrow sampling intervals as small $\delta\nu_{QCL} \sim 1$ kHz (limited by the sampling speed of the D-scope), a large number of spectral points (~10 000), and a very high SNR ($\sim 10^4$ in 10 s). Thanks to the high SNR achieved and the large number of spectral points acquired, combined to a direct measurement of the sub-Doppler profile, precise determination of spectroscopic parameters can be obtained, without any modulation-induced line-shape distortion.

IV. LOCKING SCHEME

Measurement precision, resolution, and SNR critically depend on the performance of the PLL which has to be carefully designed, independently on the chosen approach. For this purpose, we chose low-noise wide-bandwidth electronic components and we introduced a divide-by-16 digital frequency-prescaler in the control loop. We also adopted a low-noise QCL current driver (noise spectral-density as low as 3 nA/$\sqrt{\text{Hz}}$) provided with an electrical modulation input-connector with an RF bandwidth of 2 MHz. As shown in Fig. 3(a), due to the overlapping QCL and comb electric fields, a ~40 dB, ~1 MHz full-width half-maximum (FWHM) beat-note signal is detected by PD_1

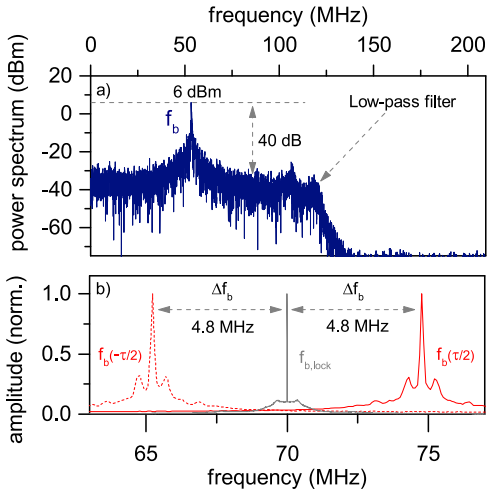

FIG. 3. (a) Low-pass filtered free-running beat note f_b in logarithmic scale (38 kHz resolution-bandwidth). (b) Linear plot of f_b tight-locked to a reference frequency of 70 MHz (f_{RF} = 60 MHz), respectively, in the case of unmodulated reference (gray line, measurement resolution-bandwidth of 3.8 kHz) and frequency-modulated reference of f_{mod} = 1 kHz and Δf_{RF} = 300 kHz (red line ~76 kHz resolution-bandwidth). A ~60% fractional spectral power was measured in the coherent peak for the unmodulated beat-note in gray. The two snapshots f_b are taken, respectively, at a delay time of $-\tau/2$ (dashed red line) and $+\tau/2$ (solid red line) with respect to the trigger instant, where $\tau = f_{mod}^{-1}$ is the modulation period.

in open-loop conditions. By adjusting the input bias current of the QCL driver, we coarsely set $f_b(t)$ to ~70 MHz. The ~70 MHz low-pass filtered and amplified beat-note $f_b(t)$ is mixed with a 890 MHz harmonic-signal provided by a low-noise RF synthesiser and upscaled to ~960 MHz; then it is frequency-divided by 16 in a digital prescaler and compared in a fast phase-frequency detector (1 MHz output bandwidth) to a f_{RF} = 60 MHz low-noise reference-signal. After being processed by a field programmable gate array based digital proportional-derivative-integrative (PID) servo, the error signal from the phase-detector is fed back to the QCL current driver. In closed loop operation, the RF spectrum of $f_b(t)$ shrinks down to below the measurement resolution and exactly at a central frequency of 70 MHz, showing the good performances of the locking-servo [gray narrow peak of Fig. 3(b)].

In order to perform CR-DFS and CR-WMS measurements, we apply a frequency modulation $\Delta f(t)$ to the reference signal f_{RF}, respectively, with triangular and sinusoidal temporal shapes, with modulation frequencies f_{mod} from 1 kHz to 100 kHz and modulation depths Δf in the 100 kHz–5 MHz range. In order to check whether $\Delta f(t)$ coherently transfers to $\nu_{QCL}(t)$, we used D-scope [triggered by $f_{RF}(t) = f_{RF} + \Delta f(t)$] to perform a sliding-window FFT analysis of the beat-note $f_b(t)$. In particular, two different snapshots of $f_b(t)$ [red peaks of Fig. 3(b)] are measured in correspondence with the minimum and the maximum of $\Delta f(t)$. The maximum measured frequency deviation Δf_b of 4.8 MHz from the 70 MHz non-modulated value is consistent with the pre-scaled maximum modulation depth of Δf = 300 kHz applied to $f_{RF}(t)$, confirming that the modulation signal is completely transferred to the QCL optical frequency (note that the ~150 kHz FWHM of the modulated beat-note is consistent with the 76 kHz resolution-bandwidth adopted for the FFT). As a result, a very accurate calibration of the instantaneous optical frequency can be achieved both in direct- and modulation-spectroscopy scans, even when modulation frequencies of few tens of kHz are applied to the QCL optical frequency.

V. SPECTROSCOPIC MEASUREMENTS

The molecular species investigated for testing the system performances is a sample of pure CHF_3 at room temperature. A pump beam intensity of 190 mW/cm^2 and a CHF_3 pressure ranging between ~1 and ~20 Pa are typically used to acquire the Lamb-dip signals.

An initial alignment optimisation and a coarse frequency calibration are done to monitor the gas absorption signal from PD_2 while sweeping the QCL current in an unlocked condition.

The free-running scan allows us to monitor the sample absorption spectra in order to maximise the saturated-absorption signal (Lamb dip), minimize alignment-related etalon effects, and choose the desired frequency window for the precision spectroscopy measurements: in particular, we focus onto the $^rR_{40}(64)$ line which is, among those with higher line-strength factor within the QCL tuning region, one of the most isolated lines. By activating the PLL, we tight-lock the QCL emission frequency to the value $\nu_{QCL} = nf_r + f_b$, with $f_r = 250$ MHz and $f_b = 70$ MHz while the exact value of the comb mode order $n = 138\,968$ is determined by the initial value of ν_{QCL} measured by the wavemeter.

We evaluated the frequency resolution in tight-locking conditions by measuring the frequency-to-intensity noise conversion on the shoulder of a saturated absorption-dip of CF_3H (Fig. 4). Such a narrow feature of ~2 MHz FWHM with a slope of ~0.15 mV/kHz allowed us to verify narrowing of the ~1 MHz free-running QCL linewidth (light-blue dotted line of Fig. 4) to ~160 kHz when the QCL is tight-locked to the comb, for 1-s integration time. We attribute this value to the frequency jitter of the mid-IR comb tooth, which in turn is ascribable to a coherent noise transfer from the RF_2 synthesizer adopted to stabilize f_r. A further improvement by a factor of ~8 of the resolution is feasible by replacing RF_2 with a synthesiser with improved noise characteristics.[21]

The precise identification of the frequency-position of the saturated-absorption dip profiles is first performed by ~1 GHz wide CR-DLS recordings at ~5 Pa pressure [Fig. 5(a)]: starting from a desired value of ν_{QCL}, at each step, f_r is incremented by a fixed amount $\delta f_r = 1$ Hz (corresponding to an optical frequency step of $\delta\nu_{QCL} = n{\cdot}f_r = 138.968$ kHz) in order to create a linear array of absolute optical frequencies. At the same time, the signal from PD_2 is acquired by the DAQ board while f_r is recorded using a 12 digit frequency counter. Each point of the scan is acquired in 1-s integration time, essentially limited by the f_r scanning speed and frequency counter measurement time, for a total acquisition time of ~1000 s per scan and a maximum SNR of $\sim 10^2$ with respect to the Lamb-dip amplitude.

CR-WMS scans are showed in Fig. 5(b). The optical modulation signal is directly applied to $f_b(t) = f_b(0) + \Delta f_b \sin(2\pi f_{mod} t)$ while the absolute optical frequency axis is again scanned by changing f_r of fixed amounts $\delta f_r = 1$ Hz. We adopted a modulation depth Δf_{mod} of 10 kHz and a modulation frequency $f_{mod} = 100$ kHz, well within the locking bandwidth of the f_b servo. After being de-modulated in a lock-in amplifier with a 300 ms integration time, the spectroscopic signal from PD_2 is acquired by the DAQ board and recorded as a function of ν_{QCL} (~160 spectral points for a total acquisition time of ~5 min per measurement).

For the CR-DFS measurements, we used a triangular modulation of frequency $f_{mod} = 1$ kHz and a depth $\Delta f_{RF} = 300$ kHz, which translates into $\Delta f_b = \pm 4.8$ MHz due to the prescaling factor of 16 [$\Delta f_b(t) = 16\Delta f_{RF}$]. The direct absorption signal from PD_2 is sent to the D-scope and recorded as a function of time after averaging. The oscilloscope time scale can be accurately and univocally remapped onto the absolute optical frequency scale using the usual formula $\nu_{QCL} = nf_r \pm f_b(t)$,

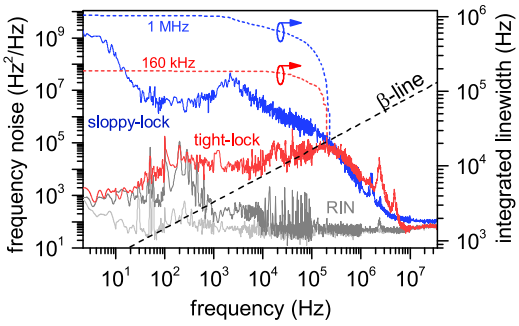

FIG. 4. Left axis: frequency noise Power Spectral Density (PSD) of the QCL in sloppy-locked (blue) and phase-locked (red) conditions, together with the RIN contribution (dark-gray), noise floor (light-gray), and β-line $8\ln 2/\pi^2 f$ (black). Right axis: calculated emission linewidth versus integration bandwidth, by means of the β-line method. PSD integration is carried out only up to frequencies below the crossing-point between β-line and frequency-noise (frequency-noise below the β-line does not contribute to the QCL linewidth[20]). The sloppy-locked integrated linewidth of ~1 MHz agrees with the ~1 MHz FWHM QCL linewidth obtained from a direct measurement of the f_b spectral-width.

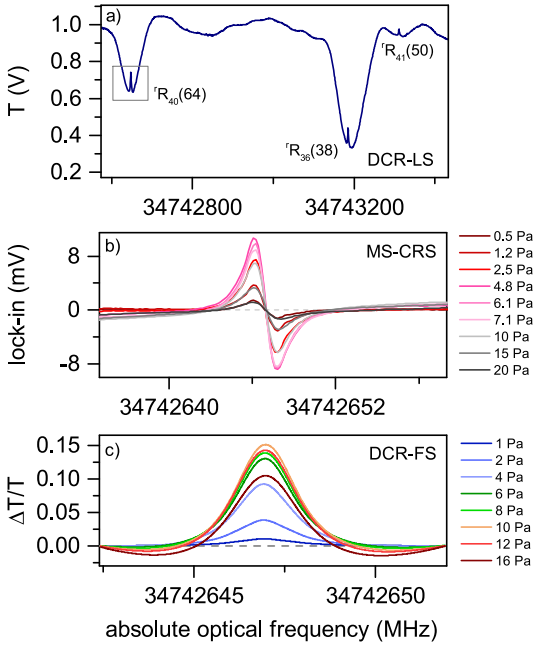

FIG. 5. (a) CR-DLS at a 5 Pa gas pressure in a ~1 GHz wide spectral window. Absorption dips of three of the strongest CHF_3 absorption features are clearly visible with a ~15% contrast. The overall wobbling trend of the spectrum, clearly observable between the two most intense lines, is due to a very large number of overlapping lines with a small absorption-intensity. (b) CR-WMS dispersive profile of the $^rR_{40}(64)$ line for several values of the gas pressure. (c) CR-DFS measurements of the $^rR_{40}(64)$ absorption line for different pressures. Curves have been normalised in order to highlight the absorption-dip contrast $\Delta T/T$ (where T is the maximum absorption of the corresponding Doppler broadened profile).

where the temporal behavior of $f_b(t)$ is precisely determined by the settings of the synthesiser generator RF_2 (Δf_{RF}, f_{mod}, function shape, and timing trigger function). Figure 5(c) reports a set of 8 measurements acquired at different pressures ranging from 1 Pa to 16 Pa. Each measurement, consisting in ~2500 spectral points, is a real-time average of 10 000 consecutive single-scans for a total acquisition time of 10 s per measurement.

CR-DFS were analyzed by fitting the saturated-absorption dip with a Voigt function. For the CR-WMS measurements, a linear combination of the zero, first, second, and third order Fourier coefficients of a Voigt function has been adopted for the Lamb-dip profile, in order to properly take into account any residual-modulation-amplitude (RAM) effect.[19] The Doppler-broadened absorption background underlying the Lamb-dip has been included in the fitting routine by adding a Gaussian contribution and its first derivative, respectively, for the direct-absorption and the modulation-spectroscopy case.

From the fit-residuals plotted in Figs. 6(a) and 6(b), a 6.8×10^3 maximum SNR and a 9.6×10^2 maximum SNR, calculated over the Lamb-dip signal amplitude, can be, respectively, estimated for the CR-DFS and CR-WMS approaches. In both cases, the maximum SNR is achieved at a pressure of 10 Pa. The residuals reveal some structures, especially in the CR-WMS measurements and more evident at low pressures, which cannot be accounted for using a simple Voigt fit of the absorption dip. The nature of such fine-structure, still under investigation, may be ascribed to a hyperfine line splitting of the CHF_3 molecule.[22]

We believe that the presence of such spectral features in the residuals, in particular, for the CR-WMS method, prevents for a precise evaluation of the pressure shift and the pressure broadening coefficients of the investigated line. The retrieved values of the $^rR_{40}(64)$ line center frequency are, respectively, 34 742 646 956(8) kHz and 34 742 646 943(10) kHz for the CR-WMS and CR-DFS methods, consistent within the statistical uncertainties of the interpolations. In the case of the less ambiguous CR-DFS measurement, by interpolating the observed Lamb-dip linewidth, Γ_{FWHM}, with the following relation: $\Gamma_{FWHM} = (\Gamma_0 + \Gamma_1 \cdot p)(1 + \sqrt{1 + \Omega_0^2/(\Gamma_0 + \Gamma_1 \cdot p)^2}$ (where Γ_0 is the transit time

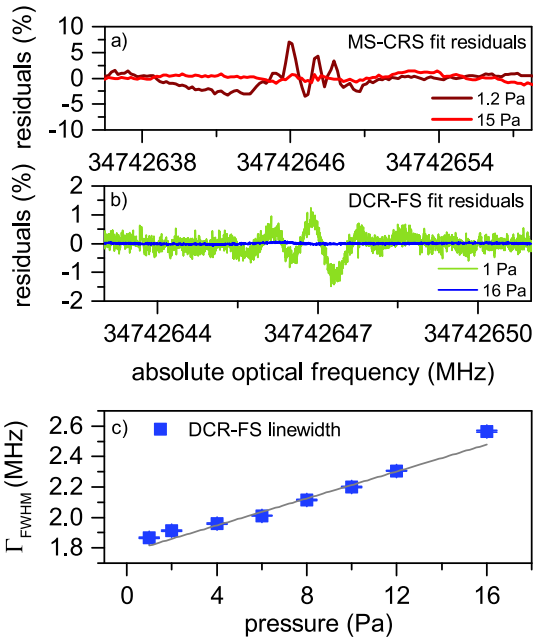

FIG. 6. Pressure dependent fit residuals for CR-DFS (a) and CR-WMS (b) measurements. (c) FWHM of the absorption dip profile as a function of the gas pressure for CR-DFS measurements (blue squares) together with the pseudo-linear fitting curve.

linewidth, Γ_1 is the pressure broadening, p is the gas pressure, and Ω_0 is the Rabi frequency),[23] we were able to evaluate the pressure-broadening coefficient of the ${}^rR_{40}(64)$ line in 35(3) kHz/Pa, with a fractional precision better than 10%.

In conclusion, we presented a versatile mid-infrared sub-Doppler comb-referenced spectrometer, capable of performing absolute frequency calibrated GHz-wide scans with a frequency resolution of ~160 kHz using three different measurement approaches in both direct spectroscopy and modulation spectroscopy configurations. Experimental validation of the spectrometer was conducted by the sub-Doppler spectroscopy of the room-temperature CHF_3 molecule. In particular, using the novel fast frequency scan direct-absorption approach, a maximum signal to noise ratio in the observation of sub-Doppler CHF_3 features of $\sim 7 \times 10^3$ for 10-s integration time was achieved underlying the spectroscopic potential of the proposed instrument.

ACKNOWLEDGMENTS

The authors acknowledge financial support from the Italian Ministry of University and Research, FIRB Project No. RBFR1006TZ, and ELI Nuclear Physics (ELI-NP) infrastructure.

[1] T. Udem, R. Holzwarth, and T. W. Hänsch, "Optical frequency metrology," Nature **416**, 233 (2002).
[2] S. A. Diddams, "The evolving optical frequency comb," J. Opt. Soc. Am. B **27**, B51–B62 (2010).
[3] T. Rosenband, D. B. Hume, P. O. Schmidt, C. W. Chou, A. Brusch, L. Lorini, W. H. Oskay, R. E. Drullinger, T. M. Fortier, J. E. Stalnaker, S. A. Diddams, W. C. Swann, N. R. Newbury, W. M. Itano, D. J. Wineland, and J. C. Bergquist, "Frequency ratio of Al^+ and Hg^+ single-ion optical clocks; metrology at the 17th decimal place," Science **319**(5871), 1808 (2008).
[4] I. Ushijima, M. Takamoto, M. Das, T. Ohkubo, and H. Katori, "Cryogenic optical lattice clocks," Nat. Photonics **9**, 185–189 (2015).
[5] J. Faist, F. Capasso, D. L. Sivco, C. Sirtori, A. L. Hutchinson, and A. Y. Cho, "Quantum cascade laser," Science **264**, 553 (1994).
[6] S. Kumar, C. W. I. Chan, Q. Hu, and J. L. Reno, "A 1.8-THz quantum cascade laser operating significantly above the temperature of $\hbar\omega/k_B$," Nat. Phys. **7**, 166 (2011).
[7] S. Bartalini, S. Borri, P. Cancio, A. Castrillo, I. Galli, G. Giusfredi, D. Mazzotti, L. Gianfrani, and P. De Natale, "Observing the intrinsic linewidth of a quantum-cascade laser: Beyond the Schawlow-Townes limit," Phys. Rev. Lett. **104**(8), 083904 (2010).
[8] A. Schliesser, N. Picqué, and T. W. Hänsch, "Mid-infrared frequency combs," Nat. Photonics **6**, 440 (2012).
[9] S. T. Wong, K. L. Vodopyanov, and R. L. Byer, "Self-phase-locked divide-by-2 optical parametric oscillator as a broadband frequency comb source," J. Opt. Soc. Am. B **27**, 876–882 (2010).

[10] F. Adler, K. C. Cossel, M. J. Thorpe, I. Hartl, M. E. Fermann, and J. Ye, "Phase-stabilized, 1.5 W frequency comb at 2.8-4.8 μm," Opt. Lett. **34**, 1330–1332 (2009).
[11] N. Coluccelli, H. Fonnum, M. Haakestad, A. Gambetta, D. Gatti, M. Marangoni, P. Laporta, and G. Galzerano, "250-MHz synchronously pumped optical parametric oscillator at 2.25-2.6 μm and 4.1-4.9 μm," Opt. Express **20**, 22042–22047 (2012).
[12] A. Gambetta, N. Coluccelli, M. Cassinerio, D. Gatti, P. Laporta, G. Galzerano, and M. Marangoni, "Milliwatt-level frequency combs in the 8-14 μm range via difference frequency generation from an Er:fiber oscillator," Opt. Lett. **38**, 1155 (2013).
[13] W. Demtröder, *Laser Spectroscopy* (Springer-Verlag, Berlin, 1982).
[14] I. D. Lindsay, P. Groß, C. J. Lee, B. Adhimoolam, and K.-J. Boller, "Mid-infrared wavelength- and frequency-modulation spectroscopy with a pump-modulated singly-resonant optical parametric oscillator," Opt. Express **14**, 12341–12346 (2006).
[15] C. Sommer, L. D. van Buuren, M. Motsch, S. Pohle, J. Bayerl, P. W. H. Pinkse, and G. Rempe, "Continuous guided beams of slow and internally cold polar molecules," Faraday Discuss. **142**, 203 (2009).
[16] A. Gambetta, E. Vicentini, Y. Wang, N. Coluccelli, E. Fasci, L. Gianfrani, A. Castrillo, V. Di Sarno, L. Santamaria, P. Maddaloni, P. De Natale, P. Laporta, and G. Galzerano, "Absolute frequency measurements of CHF_3 Doppler-free ro-vibrational transitions at 8.6 μm," Opt. Lett. **42**, 1911–1914 (2017).
[17] A. Gambetta, N. Coluccelli, M. Cassinerio, T. T. Fernandez, D. Gatti, A. Castrillo, A. Ceausu-Velcescu, E. Fasci, L. Gianfrani, L. Santamaria, V. Di Sarno, P. Maddaloni, P. De Natale, P. Laporta, and G. Galzerano, "Frequency-comb-assisted precision laser spectroscopy of CHF_3 around 8.6 μm," J. Chem. Phys. **143**(23), 234202 (2015).
[18] M. Lamperti, B. AlSaif, D. Gatti, M. Fermann, P. Laporta, A. Farooq, and M. Marangoni, "Absolute spectroscopy near 7.8 μm with a comb-locked extended-cavity quantum-cascade-laser," Sci. Rep. **8**, 1292 (2018).
[19] P. Kluczynski, J. Gustafsson, A. M. Lindberg, and O. Axner, "Wavelength modulation absorption spectrometry—An extensive scrutiny of the generation of signals," Spectrochim. Acta, Part B **56**, 1277–1354 (2001).
[20] G. Di Domenico, S. Schilt, and P. Thomann, "Simple approach to the relation between laser frequency noise and laser line shape," Appl. Opt. **49**, 4801–4807 (2010).
[21] A. Gambetta, M. Cassinerio, N. Coluccelli, E. Fasci, A. Castrillo, L. Gianfrani, D. Gatti, M. Marangoni, P. Laporta, and G. Galzerano, "Direct phase-locking of a 8.6-μm quantum cascade laser to a mid-IR optical frequency comb: Application to precision spectroscopy of N_2O," Opt. Lett. **40**, 304–307 (2015).
[22] A. W. Ellenbroek and A. Dymanus, "Molecular Zeeman effect in fluoroform and methyl chloride by beam maser spectroscopy," Chem. Phys. **35**, 227–238 (1978).
[23] V. S. Letokhov, *Saturation Spectroscopy* (Springer Berlin Heidelberg, Berlin, Heidelberg, 1976).